行政院國家科學委員會專題研究計畫　成果報告

腺核甘三磷酸感受性鉀離子通道膜內區域之表現,純化,及結晶

計畫類別：個別型計畫
計畫編號：NSC91-2311-B-002-046-
執行期間：91 年 08 月 01 日至 92 年 07 月 31 日
執行單位：國立臺灣大學醫學院口腔生物科學研究所

計畫主持人：樓國隆

報告類型：精簡報告

處理方式：本計畫可公開查詢

中　華　民　國 92 年 10 月 17 日

Structural Basis of Binding and Inhibition of Novel Tarantula Toxins in Mammalian Voltage-Dependent Potassium Channels

*Yu-Shuan Shiau[1,2], Po-Tsang Huang[2,3], Horng-Huei Liou[4], Yen-Chywan Liaw[5], Yuh-Yuan Shiau[2] and Kuo-Long Lou[2,3]**

[1]Institute of Entomology, National Taiwan University; [2]Graduate Institute of Oral Biology, Medical College, National Taiwan University; [3]Institute of Biochemistry and Molecular Biology, College of Medicine, National Taiwan University; [4]Department and Graduate Institute of Pharmacology, Medical College, National Taiwan University; [5]Institute of Molecular Biology, Academia Sinica, Taipei, Republic of China.

TITLE RUNNING HEAD: Docking of Tarantula Toxins in Kv2.1 Channels

***CORRESPONDING AUTHOR FOOTNOTE**:

Mailing Address: Dr. Kuo-Long Lou, GIOB, Chang-Teh Street #1, Taipei 10042, Republic of China. Tel:+886-2-23123456 ext. 6611/6616/7691. Fax:+886-2-23820785. E-mail address: kllou@ntumc.org.

ABSTRACT:

Voltage-dependent potassium channel Kv2.1 is widely expressed in mammalian neurons and was suggested responsible for mediating the delayed rectifier (I_K) currents. Further investigation of the central role of this channel requires the development of specific pharmacology, for instance, the utilization of spider venom toxins. Most of these toxins belong to the same structural family with a short peptide reticulated by disulfide bridges and share a similar mode of action. Hanatoxin 1 (HaTx1) from a Chilean tarantula was one of the earliest discussed tools regarding this and has been intensively applied to characterize the channel blocking not through the pore domain. Recently, more related novel toxins from African tarantulas like heteroscordratoxins (HmTx) and stromatoxin 1 (ScTx1) were isolated and shown to act as gating modifiers like HaTx on Kv2.1 channels with electrophysiological recordings. However, further interaction details are unavailable due to the lack of high-resolution structures of voltage-sensing domains in such mammalian Kv

channels. Therefore, in the present study, we explored structural observation via molecular docking simulation between toxins and Kv2.1 channels based upon the solution structures of HaTx1 and a theoretical basis of an individual $S3_C$ helical channel fragment in combination with homology modeling for other novel toxins. Our results provide precise chemical details for the interactions between these tarantula toxins and channel, reasonably correlating the previously reported pharmacological properties to the 3-D structural interpretation. In addition, it is suggested that certain subtle structural variations on the interaction surface of toxins may discriminate between the related toxins with different affinities for Kv channels. Evolutionary links between spider peptide toxins and a “voltage sensor paddles” mechanism most recently found in the crystal structure of an archaebacterial K^+-channel, KvAP, are also delineated in this paper.

INTRODUCTION

More than 70 mammalian genes encoding potassium channels have been cloned, in which four different subfamilies (Kv1, Kv2, Kv3 and Kv4) are responsible for functional voltage-dependent K^+ channels (Kv) (*1*). Kv channels are homotetramers comprising six putative transmembrane segments termed S1 through S6 in each subunit. Among them, S5 through S6 assemble the central pore domain forming the

K^+-selective ion conduction pathway (*2-4*). The first four transmembrane segments (S1-S4) of voltage-gated K^+ channels do not contribute to the simple pore, and appear to underlie their unique voltage-sensing capability (*5*). S4 is an unusual transmembrane segment that contains a large number of basic residues, which has been suggested by many studies to be strongly involved in sensing changes in membrane voltage (*6-8*).

The physiological role of the Kv channels is now better understood thanks to the discovery of animal toxins that bind to Kv channels with high affinity and specificity. The Kv2 subfamily, including Kv2.1, encodes delayed rectifier (I_K) currents (*9*). Kv2.1 is widely expressed in mammalian neurons and is present in the soma and proximal dendrites, particularly in of the hippocampus (*10*). Indirect evidence suggests a major role for Kv2.1 in the regulation of electrical transmission to and from the soma (*10*). However, the specific contribution of Kv2.1 to delayed rectifier currents in neurons has not been properly investigated until recent years because of a lack of suitable pharmacological effectors. Regarding this, more emphasis has been put on the value of spider venoms as unique sources of toxins for Kv2.1 channels (*11*). Hanatoxins were first discovered to show specific inhibition on Kv2.1 through a region other than the pore domain (*12,13*). Such toxins act on the C-terminal residues of S3 segment ($S3_C$) in Kv2.1 as binding target (*14,15*) and

therefore change the channel gating towards its depolarization state (*11-13*). With the availability of a solution structure for hanatoxin 1 (HaTx1) (*16*), detailed approaches have revealed the possibility of conformational change for $S3_C$ helix in Kv2.1 interfering with the spatial freedom of S4 translocation during gating upon HaTx1 binding (*17,18*). All this confirms and emphasizes the importance of an individual $S3_C$ helix in voltage sensing and in gating (*19*), as well as toxin binding and regulation.

Recently, more novel spider toxins have been identified from the venoms of African tarantulas *Stromatopelma calceata* (for stromatoxin, ScTx1) and *Heteroscordra maculata* (for heteroscordratoxins, HmTx1; HmTx2) (*20*). The first two of these three toxins (ScTx1 and HmTx1) showed strong inhibition on Kv2.1 currents with affinity (*20*) as high as hanatoxins (*11*), whereas the last (HmTx2) only showed minor inhibition (*20*), despite the high sequence homology and a similar pattern of disulfide linkage for all three toxins. How do these tarantula toxins interact with Kv2.1? Do they exert themselves exactly in the same way as hanatoxin does to bind on $S3_C$ helix? Are they using similar structural components for their modes of action? Due to the lack of channel structures in high resolution for Kv2.1, such questions can not be answered very easily if one only relies on electrophysiological analyses. Therefore, in order to obtain structural details with which to elucidate possible molecular mechanism, we performed docking simulations for the tarantula

toxins with Kv2.1 channels. This was based upon the hypothesis that they may all use the highly conserved individual $S3_C$ helix as a binding target for the inhibition of Kv2.1 currents. Other possible mechanisms were considered as well. Our data successfully suggest a coincidental structural-functional correlation to explain the pharmacological properties previously reported (*20*). Meanwhile, such structural information may also account for the discrimination in the inhibitory behaviors between HmTx1 and HmTx2. Our data are very useful in exploring future experimental approaches to elucidate further mechanism in molecular and atomic levels. Finally, a structure model derived from KvAP crystal structure (*31*) for Kv2.1 was generated and simulated with hanatoxin as ligand.

EXPERIMENTAL METHODS

Structure of drk1 channel /$S3_C$ fragments.

The human Kv2.1 (*drk1*) $S3_C$ molecule (Val-271 to Gln-284, amino acid sequence: VTIFLTESNKSVLQ) was constructed via modification from fragment dictionary with geometry optimized using the consistent valence force field (CVFF) with Biopolymer module of Insight II software package (Accelrys, USA). Atomic charges were computed using the semi-empirical MOPAC/AM1 method. The residues

based on existence of an α-helix were individually regularized by energy minimization to give reasonable geometry.

Homology models of *drk1* channel were built up based upon coordinates from crystal structure of KvAP channel (PDB ID: 1ORQ and 1ORS) (*30-32*) (see below). Essentially, potassium voltage-gated channel subfamily B member 1 (Kv2.1, h-DRK1; NCB accession number: AAB88808) from human as search sequence was applied for homology modeling. Voltage-sensor paddle in model structure: drk1, Leu-175 to Gln-427, compared to Val-275 to Gly-316 in KvAP.

Toxin structures.

The coordinates for HaTx1 structure were obtained from Brookhaven Protein Databank in pdb file (PDB ID number 1D1H; solution structure by NMR method) (*16*). Structures for ScTx1 and HmTx1 were created via homology modeling based on the HaTx1 structure as template. HmTx2 was created by following the same procedure with ω-grammotoxin SIA (GsTxSIA, PDB ID: 1KOZ_A) (*33*) as template according to their BLAST search results (see following section).

Homology modeling of drk1, HmTx1, HmTx2 and ScTx1.

Search for templates. BLAST algorithm was employed to search in PDB the protein segments whose sequences are similar to those of tarantula toxins and whose structures can serve as viable structural templates. The crystal or solution structures of such template that showed the highest scores in the sequence alignments were chosen for the determination of structural conserved regions (SCRs). The residues of toxins used for model building are according to their paired sequence compared to the template sequence.

Paired sequence alignment. GCG program was used to determine the equivalent residues. The residue regions of template toxins represented as continuous lines dominantly observed from GCG results were employed as appropriate regions, and the corresponding fragments in the target toxins were chosen for alignment individually. The amino acid sequences of these novel toxins were then included in the multiple sequence alignment (*21*) of the appropriate template regions to specify the residue numbers for model building.

Model building and residue side-chain simulation. Modeling by homology was performed essentially following the procedures previously described (*21-25*). Briefly, the residue fragments of novel toxins were chosen according to the results from GCG paired sequence alignment. They were then superimposed onto the structure coordinates of Cα atoms of the corresponding SCRs from template toxin structure.

This generated the secondary structure and relative position of the definite structural elements in the chosen residue fragments of individual target toxin models. Junctions between the secondary structural elements were individually regularized by energy minimization to give reasonable geometry. Further hydrophobic/-philic interactions between residue side-chains were performed and obtained with molecular dynamics and simulated annealing. All the calculations and structure manipulations were performed with the Discover/Insight II molecular simulation and modeling programs (from Accelrys Inc., San Diego, CA, USA; 950 release) on Silicon Graphics Octane/SSE and O2/R12000 workstations as well as O-300 server.

Docking Simulation.

Determination of starting orientations. In principle, three criteria were used to determine the starting positions: stereochemistry, side-chain charge distribution, and previous structural information (*16-20*). Inappropriate possibilities have been immediately excluded when definitely unreasonable combinations of alignment for docking were observed. Uncertain orientations were reserved and submitted for docking calculation to allow the computational results to perform the screening.

Calculation for the energies. Upon docking, the total energies of electrostatic interactions and van der Waals contacts between the complexes of novel tarantula

toxins and $S3_C$ (binding models) were compared. Each run was composed of 500 cycles of simulated annealing and 500,000 steps of accepted/rejected configurations.

The values of all other default parameters were used. The alignment between docked and undocked molecules was performed by manually fitting the atomic coordinates of groups of residues that may be involved in the conserved interaction (*17,19*). Briefly, three-dimensional (3D) surfaces of the binding site enclose the most active members (after appropriate alignment) of the starting set of molecules. Note that errors in alignment can lead to incorrect, poorly predictive receptor surface models. This problem was overcome by using information obtained from previously related functional data (*19,20*). The surface was generated from a "shape field", in which the atomic coordinates of the contributing models were used to compute field values on each point of a 3D grid using a van der Waals function (*26-28*). A solvation energy correction term and the electrostatic charge complementarity's method were used for energy evaluation (*26,27*). And with that, the solvation energy correction term is a penalty function that attempts to account for the loss of solvation energy when polar atoms are forced into hydrophobic regions of the receptor surface. All the calculations and structure manipulations described above were performed with the Discover & Docking/Insight II (2000) molecular simulation and modeling program

(Accelrys, San Diego, CA, USA; 950 release) displayed on a Silicon Graphics O2/R12000 and Octane/SSE workstations.

THEORETICAL BASIS

Molecular and docking simulation has since more than a decade been contributing to precise interaction details in atomic levels, provided an appropriate force field is applied. However, the accurate structural information will be ensured and reliable only when the starting orientations and positions are correctly determined. For such reason, distinguished strategies to perform simulations are undoubtedly crucial and absolutely required to be established before the docking procedure commences. Sufficient constraints based on the previous functional properties will assist this to a fairly large extent. In our case, as also described in the methods section, the hydrophobic patch and the charged belt of these toxins are sufficient as criteria in both stereochemistry and previous functional data. Thus all the rest is to observe and make decisions for the best combination possibilities within a restricted area by rotation and/or translocation of the receptor/ligand molecules, especially for residue side chains, and then to allow the energy results to be compared. In addition to such

important starting point, the other pivotal concept for how to take free body of the interaction system is described in the next paragraph.

Many tarantula toxins as hanatoxins bind and inhibit mammalian Kv channels not through the pore domain. The carboxyl terminal residues of the transmembrane segment S3 are highly conserved in voltage-dependent potassium channels and have been suggested for such target of binding sites. However, due to the lack of high-resolution structure for voltage-sensing domains before in previous stage, docking simulation for this kind of toxin-channel interaction was thought to be either impossible or with less significance. Recently, mutagenesis scanning and helical analyses (*19,29*) as well as other previous progresses, which led to the observation that $S3_C$ should be regarded as an individual helical fragment, have provided us the opportunity to consider this interaction system as a free body, and therefore the molecular simulation could be performed within this space. Furthermore, simulation results would provide compensation through comparison of the energy states even if this helix has distortion in three dimensions. We have tested this idea with a system containing hanatoxin and *drk1/shaker* $S3_C$ (*17,18*). Chemical details of interaction correlated successfully in both structural and functional aspects (*17,19*). Spatial orientation of $S3_C$ helix was appropriately discussed (*18*) and even structural change of molecules, as well as interference in spatial freedom, could be comprehensively

analyzed through our simulation results (*17,18*). Moreover, existence of $S3_C$ helix as individual fragment seemed to have been strongly confirmed as a result of low energy for binding. Thus, the expansion of such a concept into the interactions between various members in tarantula toxin family and mammalian channels in this study is supposed to be quite rational. Meanwhile, the related algorithms and functions applied in the simulation procedures are described in detail in the Experimentals section.

The crystal structures of a voltage-gated potassium channel from thermophilic archaebacteria (*30*) have been quite recently determined to atomic resolutions (*31*). A mechanism for gating based upon “voltage-sensor paddles” was proposed through the structural observation (*31,32*). This mechanism gave new directions and possibilities for further investigations by considering the toxins and entire “paddle” together as an interaction free body.

RESULTS AND DISCUSSIONS

Structure of novel tarantula toxins.

In order to perform the docking simulation, the atomic coordinates of toxin structures in three dimensions are required to be assigned as receptor or ligand involved in the interactions. The solution structure of HaTx1 was used as template in

homology modeling for HmTx1 and ScTx1. The structures of template toxin and targets are compared in Fig. 1.

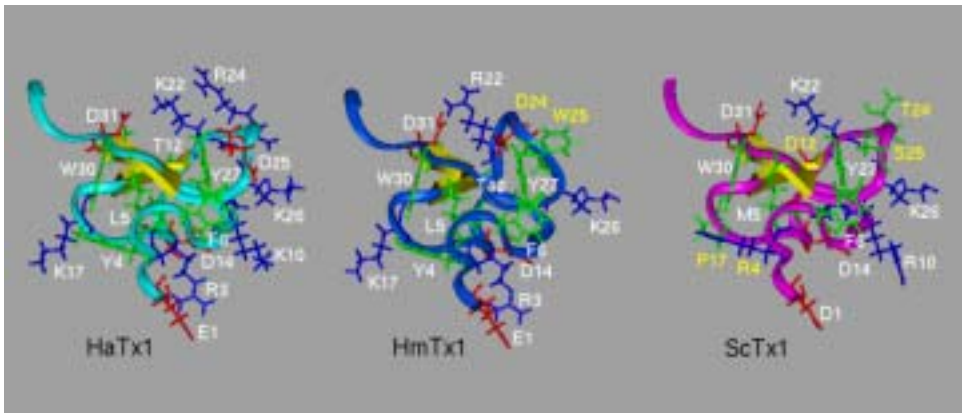

Fig. 1a

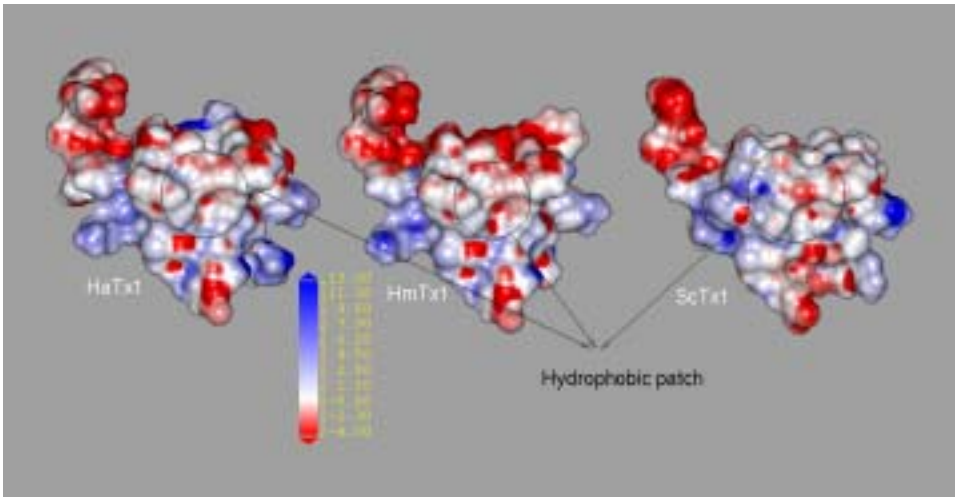

Fig. 1b

In addition to the crucial residues that may be involved in the toxin-channel binding illustrated in Fig. 1a, the charge distributions of HaTx1, HmTx1 and ScTx1 are represented with the electrostatic surface in Fig. 1b. Compared with HaTx1, the hydrophobic patch is apparently well conserved in HmTx1 and ScTx1. It is also fascinating to note that residues tending to form a charged belt, as seen in HaTx1, are also flanking the corresponding hydrophobic patch exactly in the same way and as conservative substitutions in HmTx1 and ScTx1.

HmTx2 was not suggested for the similar modeling procedure via using HaTx1 as template. Instead, BLAST results revealed a preference for GsTxSIA (*33*) as template. Comparing Fig. 1a with Fig. 2a, a major difference can be easily observed between the two sets of models.

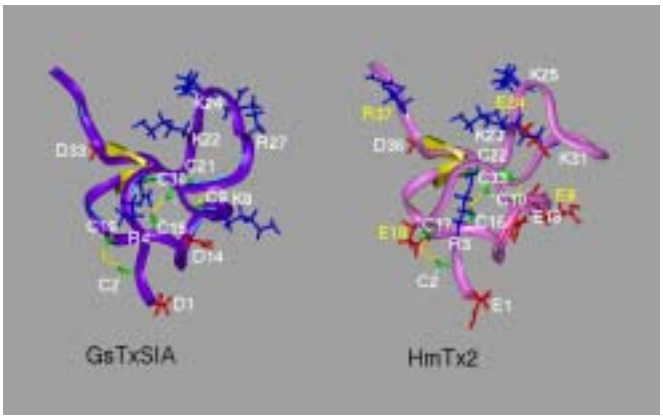

Fig. 2a

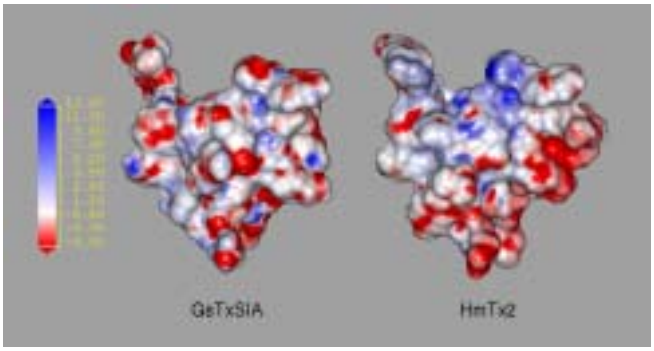

Fig. 2b

In the HmTx2 structure, a longer protruding loop containing residues 25-31 was observed (Figs. 2a-b). This fact leads to two significant consequences: (i) HmTx2 was suggested to be an inappropriate target for template HaTx1 in homology modeling; (ii) Apparent disturbance in binding for inhibition on Kv2.1 gating currents may occur. We will come back to this point in more details later in this section.

Interactions of novel toxins and a channel fragment.

In Fig. 3, the most reasonable docking results between novel toxins (ScTx1, HmTx1, and HmTx2) and channels are illustrated in comparison with the HaTx1-Kv2.1 $S3_C$ interaction. Total binding energies are listed in Table 1. All the first three complexes (Figs.3a-3c: HaTx1-, HmTx1-, and ScTx1-Kv2.1 $S3_C$, respectively) demonstrate a very similar binding mode: the residues on the hydrophobic patch of the toxin (e.g., Tyr-27 in Fig. 3a) form hydrophobic interactions with non-polar residues from Kv2.1 $S3_C$, whereas polar residues on $S3_C$ form hydrophilic interactions with residues from the charged belt flanking the patch on toxin surface. In comparison with the interaction details in Table 1, it is interesting to note that the magnitudes of inhibition (some are represented as IC_{50}) by various toxins are in line with the binding energies, which are further explained by the strength of interaction categorized as number of bonds/interactions formed by residues from both sides of participating molecules (Table 1). HaTx1 and ScTx1 both show very strong inhibition on Kv2.1 currents, therefore a reasonable docking for them should be implied from lower total binding energies, which have been successfully and clearly indicated by our simulation results (Fig. 3 and Table 1).

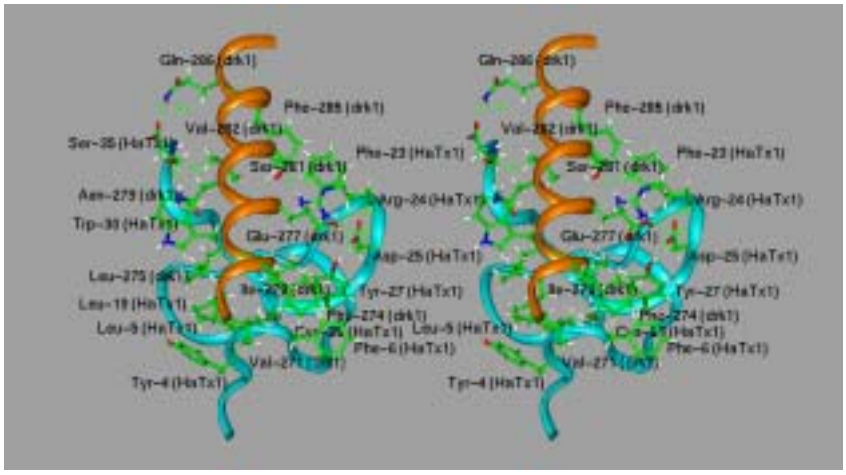

Fig. 3a

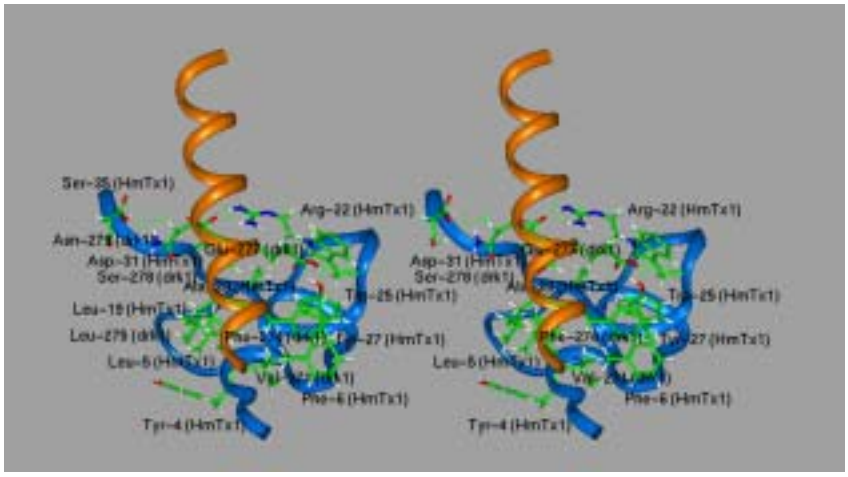

Fig. 3b

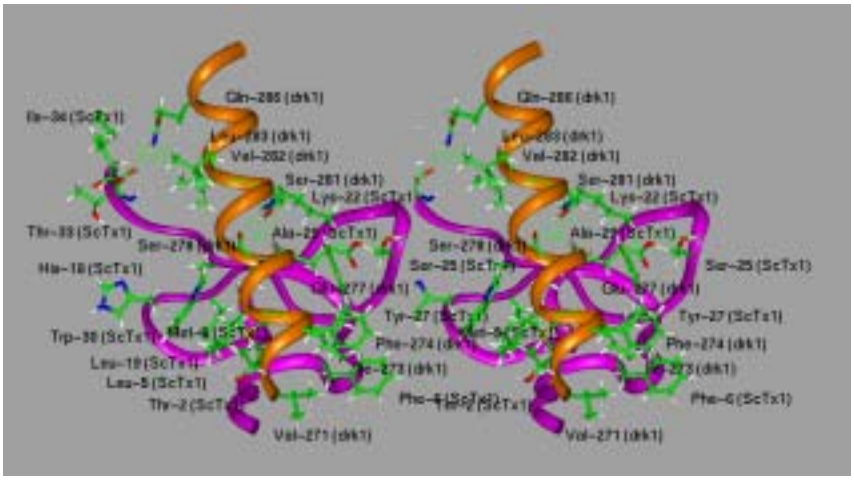

Fig. 3c

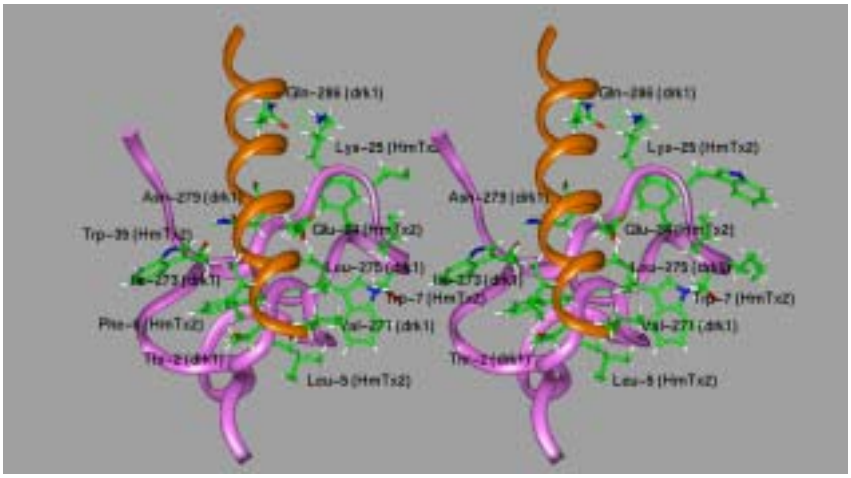

Fig. 3d

	Activity of spider toxin against *drk1* channel as IC_{50} (nM) or percent-age of current inhibition (*20*)	Van der Waals / Electro-static / Total energies (Kcal/mol) after docking	Number of Salt-bridges and H-bonds	Number of resi-dues forming hy-drophobic inter-actions
ScTx1- *drk1* $S3_C$	**12.7**	**322.05 / -219.183 / 102.87**	**6**	**15**
HaTx1- *drk1* $S3_C$	**42**	**268.85 / -35.71 / 233.14**	**7**	**14**
HmTx1-*drk1* $S3_C$	**23% (100nM)**	**402.27 / -65.20 / 337.07**	**5**	**10**
HmTx2-*drk1* $S3_C$	**18% (300nM)**	**1343.16 / -419.74 / 923.421**	**4**	**8**

Table 1

Interaction of HmTx2.

The extraordinarily weaker interactions observed for HmTx2 can be reasonably illustrated with its structural characteristics. As mentioned before, the

existence of a longer protruding loop 25-31, compared to HaTx1, ScTx1 and HmTx1, makes HmTx2 itself very distinct in shape from others (Figs. 1 & 2). When the toxins are bound onto the channel by interacting with $S3_C$ fragment, this part may become an obstacle for HmTx2 to approach towards $S3_C$. In other words, this loop will form steric hindrance to prevent a tight binding while approaching the channel. From the complex structure of HmTx2 and Kv2.1 $S3_C$ depicted in Fig. 3d, one can easily find that the longer 25-31 loop interferes with the binding of the two molecules not only through steric hindrance regarding the main bodies, but also through perturbation of residue types for detailed interaction. And therefore, the docking energies will certainly not favor HmTx2 with binding to Kv2.1 (Table 1). This concept can be further emphasized by the reduced number of residues involved in forming hydrophobic interactions compared to those for HmTx1 and ScTx1. However, the electrostatic energy is very low for HmTx2 regarding binding with Kv2.1 $S3_C$, despite that it can be compensated by the extremely high van der Waals' energy and thus produced much higher total energies. This seems to contradict the concept described previously. Therefore, we examined the complex structure of HmTx2-S3c in more details.

If one looks into the complex structure in Fig. 3d even more carefully, it is not difficult to obtain two interesting features. The first is an obvious unorganized spatial

relationship for residue side chains around the hydrophobic patch (Fig. 3d). This brings the van der Waals' energy to the very high value listed in Table 1. Another disturbing factor affecting hydrophobic interactions can be observed in the Loop 25-31 for residues adjacent to Lys-25. At this position, $S3_C$ provides several polar or charged residues to form H-bonds or salt-bridges with polar residues from toxins for HaTx1, HmTx1 and ScTx1. However, in HmTx2, a few aromatic residues are located nearby, and as a consequence, van der Waals' energy could be brought to an even higher value (Fig.3d). The second feature is with respect to the "high-positional" salt bridge (Lys-25 from HmTx2 and Gln-286 from *drk1* $S3_C$). This unusual interaction, due to the longer loop protruding from the Lys-25 side chain on tip of loop to a height about to form interaction with Gln-286 from almost the C-terminal end of $S3_C$ has not been seen in all other toxin-channel complexes (Figs. 3a-c). It might provide a rational explanation for such an unexpected low electrostatic energy listed in Table 1. Considering as a whole, the docking interaction between HmTx2 and Kv2.1 should be inappropriate or unnatural, although such orientation was the best possibility we could find to carry out simulation for this combination. The sequence of HmTx2 seems not to be designed by nature to inhibit Kv2.1 through binding on $S3_C$.

This discussion provides an explanation for the highest energy result in Table 1 for HmTx2, if compared with other novel tarantula toxins. However, should this not

also imply the possibility for a totally different orientation for binding? Conservation of the hydrophobic patch and the charged belt in HmTx2 seems to suggest a similar binding mode as observed in all the other tarantula toxins acting on $S3_C$. O*n* the other hand, evolutionary links delineated in Fig. 4 might support the point that a different kind of channel serves as binding target for HmTx2, with only subtle structural changes on $S3_C$. And this may reflect the adaptation of toxins in evolution for various environments, based on the relationship in the phylogenic tree (more close to GsTxSIA, Fig. 4b). This assumption remains to be verified through more experiments in electrophysiology. Nevertheless, the close relation between HaTx, ScTx, and HmTx1 illustrated in Fig. 4, rather than with HmTx2, indeed accounts for their pharmacological properties (*20*) and the structural observation described in this study.

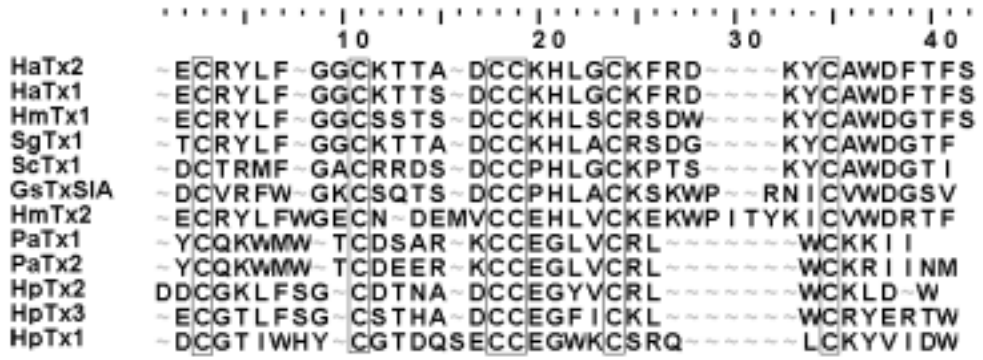

Fig. 4a

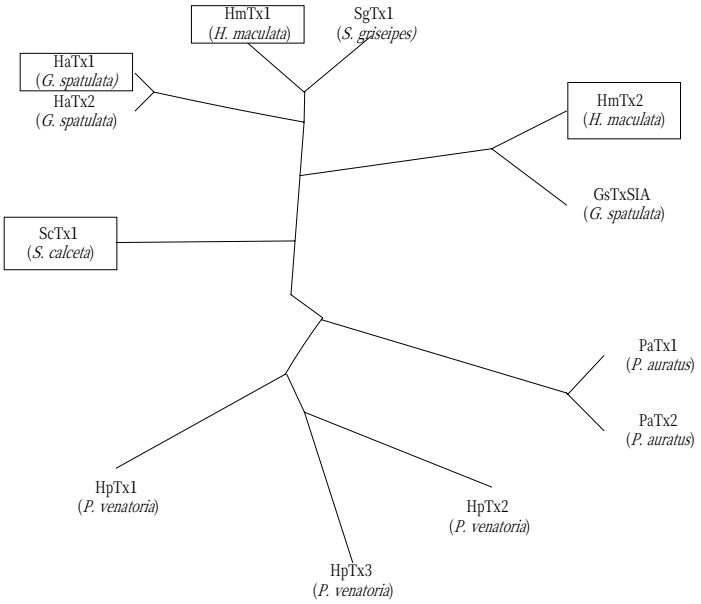

Fig. 4b

Evolutionary links.

Fig. 4a represents the sequence comparison for related tarantula toxins. Apparently the typical structural arrangement for such small peptide toxins is strictly and extensively conserved throughout widely spread species as toxin sources based on the disulphide linkage. This has been known for the Cysteine-rich proteins superfamily (*34-38*). In addition, the charged/polar residues required for the charge belt and aromatic/hydrophobic ones for the hydrophobic patch are also highly conserved in all the related spider toxins (Fig. 4a). Using ClustalW (*39*) by manual and Bioedit (*40*), a phylogenic tree, based on comparison of amino acid sequences for such related tarantula toxins delineated in Fig. 4a, can be generated (Fig. 4b). HaTx1, HaTx2, ScTx1 and HmTx1 are all located on the left top of the tree with a

neighboring branching between ScTx1 and the others. Meanwhile, HmTx2 deposits itself on the other side of the tree, even though it comes from the same venom source as HmTx1 does. This may probably conduct the structural role of a molecule into its evolutionary necessity: even a subtle change in structure (here, a small part on the interaction surface) could presumably suffice to satisfy the demands of selection.

Speculations for putative mechanism.

Previously, we have proposed a hypothesis describing a possible molecular mechanism for how hanatoxin may affect the gating behavior of Kv2.1 channels via binding on $S3_C$ fragment (*17*,*18*). In this hypothesis, we derived a C-terminal helical movement of *drk1* $S3_C$ (*17*,*18*) through observed conformational change (*17*) and binding pocket (crevice) analysis (*24*) from simulation data, reducing the spatial freedom for S4 translocation (*18*), and therefore a more depolarized potential for the open gate may arise as anticipated (*11*,*20*). However, most recently, Jiang and MacKinnon disclosed a crystal structure and therefore the principle of voltage gating of an archaebacterial K-channel, KvAP was proposed (*30*-*32*). This has a significant impact on our hypothesis. The major challenge was based on the observation that S3b (i.e., $S3_C$) and S4 (or $S4_N$) should "translocate" as an unity upon voltage-sensing and the resulting electric field, and just like a "paddle" (totally 4 paddles in one molecule).

From such a point of view, a short S3-S4 linker will be absolutely required, considering the free energy for an *en bloc* movement. This is true for the situation in KvAP (*30,31*), but not necessarily for mammalian channels, as suggested by their much more complicated kinetics and regulatory behaviors (*18,41*). To compare these two different ideas, we have carried out homology structural modeling and re-performed the docking simulation of *drk1* complexed with hanatoxin (Fig. 5). Although it is still difficult to have successful interpretation of how flexible this linker is during activation, we found a very interesting structural essential in the $S3_C$ helix (Fig. 5c): the helical arrangement becomes a random coil after the mid-point of $S3_C$. In addition, this feature seems not to interfere with the toxin binding (Fig. 5a, b). This new finding is based on energy minimization results from both modeling and docking procedures, and the reasons could be possibly comprehended in the following ways. First, it may be only due to the energy minimization similar as in a flexible loop. We would not be satisfied by such simple explanation. Second, it can reflect a compromised transitional structure preceding the S3-S4 linker in a more dynamic way, which was thought to be extremely crucial in the regulation of activation kinetics (*41*). Such a point of view may partially support our previously observed conformational change (*17,18*) in a more preserved manner, because a longer S3-S4 linker either found in *drk1* or in *shake*r should be able to provide higher spatial freedom in

regulation and thus allow a certain range of motions. We would not speculate further the role of this looser structural arrangement with such limited data. Nevertheless, all the issues discussed above may provide hints that there is still quite a large space for researchers to work on regarding the regulatory roles of the area around the vicinity of $S3_C$ and $S4_N$. In other words, it is not an ending, but on the contrary, just a fresh beginning for further investigations after the unraveling of this first crystal structure of an archaebacterial Kv channel containing the whole voltage-sensing domains. And for tarantula toxins, they will be even more useful in the future study of the related gating phenomena they have shown to us in the past decade.

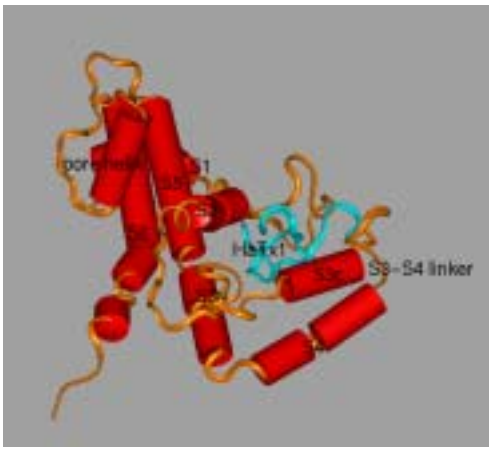

Fig. 5a

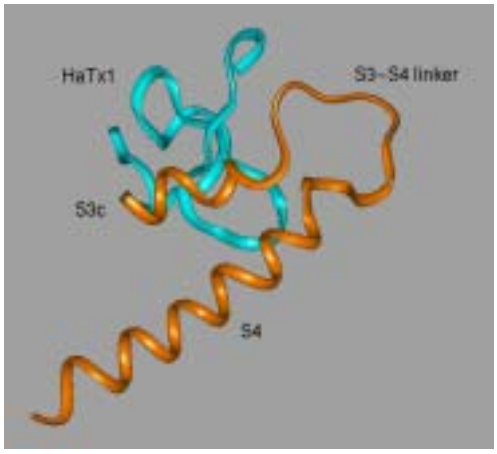

Fig. 5b

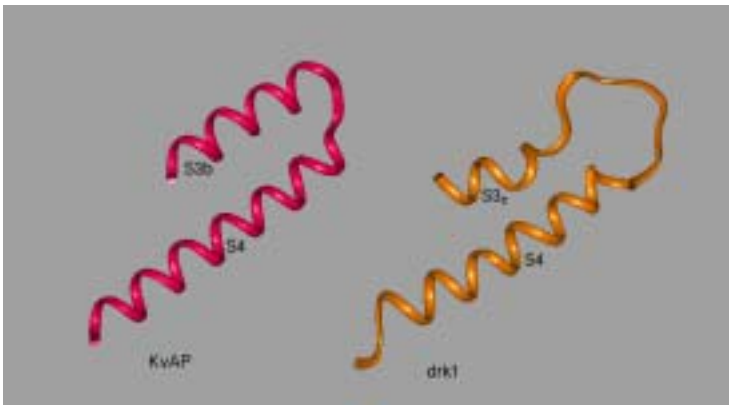

Fig. 5c

Conclusion. Based upon an *in silico* study, we have provided a structural basis for the inhibition and binding of mammalian Kv channels by novel tarantula toxins, successfully correlating their previously reported pharmacological properties to a 3-D structural-functional interpretation. By combining this structural model with evolutionary considerations, discrimination between subtypes of toxins due to subtle structure changes in the interaction surface can be proposed. Finally, a "voltage-sensor paddles" mechanism deduced from the crystal structure of archaebacterial channel has been used as reference for further consideration on toxin-channel behavior in mammalian Kv channels.

ACKNOWLEDGEMENT. The authors thank Dr. Wang Pao-Hsiang at Dept. of Foreign Languages and Literature in NTU with deepest sincerity for his careful reading through the manuscript and his useful suggestions in further correction of the sentences. This work was supported in part by the Taiwanese NSC fundings 92-2914-I-002-077-A1/91-2914-I-002-191-A1 and the Grants 912C012/902A006 and 92G017 from Teaching Improvements Projects Package by AOE, R.O.C. for LKL.

FIGURE CAPTIONS

Figure 1. Comparison for overall structures of novel tarantula toxins: HaTx1, HmTx1, and ScTx1. (a) Ribbon diagrams for template structure of HaTx1 and homology structure models of HmTx1 and ScTx1. Crucial residue side chains that may involve in the interaction with channels are emphasized with residue number indicated. Residues in HmTx1 and ScTx1 structures not appearing as conservative substitutions are labeled in yellow (otherwise in white). **(b)** Electrostatic surface of novel toxins. Approximate locations for the hydrophobic patch are marked with

circles in black. On the surface of molecules, red corresponds to an electrostatic potential of $\leq$ -4.0 k_BT/e, white to 0 k_BT/e, and blue for $\geq$3.0 k_BT/e.

Figure 2. Comparison of overall structures of novel tarantula toxins: HmTx2 and GsTxSIA. As shown in Fig.1, the schematic diagrams for both template GsTxSIA and target HmTx2 are illustrated in **(a)** with crucial residue side chains opened and residue types, number emphasized; **(b)** Electrostatic surface potentials represented: red for $\leq$ -4.0 k_BT/e, white for 0 k_BT/e, and blue for $\geq$ 13.0 k_BT/e.

Figure 3. Stereo views for complex structures of various tarantula toxins and *drk1* $S3_C$ from docking simulation results. **(a)** HaTx1-$S3_C$ (cyan), **(b)** HmTx1-$S3_C$ (dark blue), **(c)** ScTx1-$S3_C$ (magenta), and **(d)** HmTx2-$S3_C$ (violet). Kv2.1 $S3_C$ is colored in orange. Crucial residue side chains involved in the interactions are opened and drawn in colors according to their atom types with residue number indicated. It is important to note that in Fig. 3d, a distinct longer Loop 25-31 in HmTx2 displays an unusual structural characteristics regarding steric hindrance for binding (see text for more details).

Figure 4. Evolutionary links between related tarantula toxins. (a) Sequence alignments. **(b)** Phylogenic tree. Software used to produce these figures has been described in detail in the Methods section.

Figure 5. Further study of HaTx1-Kv2.1 interaction based on crystal structural information from archaebacterial KvAP channel. (a) Overview of Kv2.1 (*drk1*) structure in complex with HaTx1. Homology structures for *drk1* were generated as described in Experimental section. Red cylinders represent the α-helices. Connection loops are built up with yellow ribbons with energy minimization to give reasonable geometry. HaTx1 molecule is shown in blue. **(b)** Enlarged view for *drk1* voltage-sensor paddle in ligand with HaTx1. **(c)** Comparison of voltage sensors between KvAP and Kv2.1 (*drk1*). Close attention is suggested for the different structural arrangement in the C-terminal part of $S3_C$ (or S3b) (see more details in text). Residues applied: Pro-99 to Ala-140 in KvAP, whereas in Kv2.1, Val-275 to Gly-316. Besides, gap in modeling was suggested between Gly-114 and Leu-115 in KvAP for S3-S4 linker in *drk1* replaced by residues between Leu-287 and Val-295. All the structural manipulations were performed with Insight II software package as described in Experimental section.

TABLES.

Table 1. Comparison of the magnitudes of inhibition by novel tarantula toxins on *drk1* currents with the structural features (energies, bonds, etc.) after docking calculations.

REFERENCES

(1) Jan, L. Y., and Jan. Y. N. (1997) Cloned potassium channels from eukaryotes and prokaryotes. *Annu. Rev. Neurosci.* **20**, 91-123.

(2) Liman, E. R., Tytgat, J., and Hess, P. (1992) Subunit stoichiometry of a mammalian K^+ channel determined by construction of multimeric cDNAs. *Neuron* **9,** 861-871.

(3) Heginbotham, L., Lu, Z., Abramson, T., and MacKinnon, R. (1994) Mutations in the K^+ channel signature sequence. *Biophys. J.* **66,** 1061-1067.

(4) Ranganathan, R., Lewis, J. H., and MacKinnon, R. (1996) Spatial localization of the K^+ channel selectivity filter by mutant cycle-based structural analysis. *Neuron* **16**, 131-139.

(5) Armstrong, C. M. and Hille, B. (1998) Voltage-gated ion channels and electrical excitability. *Neuron* **20,** 371-380.

(6) Bezanilla, F., Perozo, E., Papazian, D. M., and Stefani, E. (1996) Molecular basis of gating charge immobilization in *shaker* potassium channels. *Science* **254,** 679-83.

(7) Cha, A., Snyder, G. E., Selvin, P. R., and Bezanilla, F. (1999) Atomic scale movement of the voltage-sensing region in a potassium channel measured via spectroscopy. *Nature* **402,** 809-813.

(8) Bezanilla, F. (2000) The voltage sensor in voltage-dependent ion channels. *Physiol. Rev.* **80**, 555-592.

(9) Frech, G. C., van Dongen, A. M., Schuster, G., Brown, A. M., and Joho, R. H. (1989) A novel potassium channel with delayed rectifier properties isolated from rat brain by expression cloning. *Nature (Lond)* **340**, 642-645.

(10) Murakoshi, H. and Trimmer, J. S. (1999) Identification of the Kv2.1 K^+ channels as a major component of the delayed rectifier K^+ currents in rat hippocampal neurons. *J. Neuronsci.* **19**, 1728-1735.

(11) Swartz, K. J., and Mackinnon, R. (1995) An inhibitor of the Kv2.1 potassium channel isolated from the venom of a Chilean tarantula. *Neuron* **15,** 941-949.

(12) Swartz, K. J., and Mackinnon, R. (1997) Hanatoxin modifies the gating of a voltage-dependent K^+ channel through multiple binding sites. *Neuron* **18,** 665-673.

(13) Swartz, K. J., and Mackinnon, R. (1997) Mapping the receptor site for hanatoxin, a gating modifier of voltage-dependent K^+ channels. *Neuron* **18,** 675-682.

(14) Rogers, J. C., Qu, Y., Tanada, T. N., Scheuer, T., and Catterall, W. A. (1996) Molecular determinants of high affinity binding of alpha-scorpion toxin and sea anemone toxin in the S3-S4 extracellular loop in domain IV of the Na^+ channel alpha subunit. *J. Biol. Chem.* **271,** 15950-15962.

(15) Winterfield, J. R. and Swartz, K. J. (2000) A hot spot for the interaction of gating modifier toxins with voltage-dependent ion channels. *J. Gen. Physiol.* **116,** 637-644.

(16) Takahashi, H., Kim, J. I., Min, H. J., Sato, K., Swartz, K. J., and Shimada, I. (2000) Solution structure of Hanatoxin1, a gating modifier of voltage-dependent K^+ channels: common surface features of gating modifier toxins. *J. Mol. Biol.* **297,** 771-780.

(17) Huang, P.-T., Liou, H.-H., Lin, T.-B., Shiau, Y.-S., Spatz, H.-Ch., Chen, T.-Y., Tzeng, L.-J., Shiau, Y.-Y., and Lou, K.-L. (2001) Structural influence of

hanatoxin binding on the carboxyl terminus of S3 segment in voltage-gated potassium channel Kv2.1. *Recept. Channels* **8**, 79-85.

(18) Lou, K.-L., Huang, P.-T., Shiau, Y.-S., French, R. J., Liaw, Y.-C., Shiau, Y.-Y., and Liou, H.-H. (2003) A possible molecular mechanism of hanatoxin binding-modified gating in voltage-gated potassium channels. *J. Mol. Recognit.* (in press).

(19) Li-Smerin, Y., and Swartz, K. J. (2001) Helical structure of the COOH terminus of S3 and its contribution to the gating modifier toxin receptor in voltage-gated ion channels. *J. Gen. Physiol.* **117,** 205-218.

(20) Escoubas, P., Diochot, S., Célérier, M.-L., Nakajima, T., and Lazdunski, M. (2002) Novel tarantula toxins for subtypes of voltage-dependent potassium channels in the Kv2 and Kv4 subfamilies. *Mol. Pharmacol.* **62**, 48-57.

(21) Voorhorst, W. G., Warner, A., de Vos, W. M., and Siezen, R. J. (1997) Homology modelling of two subtilisin-like proteases from the hyperthermophilic archaea *Pyrococcus furiosus* and *Thermococcus stetteri*. *Prot. Engineer.* **10**, 905-914.

(22) Tsai, Y.-W., Chia, J.-S., Shiau, Y.-Y., Chou, H.-C., Liaw, Y.-C., and Lou, K.-L. (2000) Three dimensional modeling of the catalytic domain of S. mutans glucosyltransferase B. *FEMS Microbiol. Lett.* **188**, 75-79.

(23) Lou, K.-L., Chou, H.-C., Tsai, Y.-W., Shiau, Y.-S., Huang, P.-T., Chen, T.-Y., Shiau, Y.-Y., and French, R. J. (2001) Involvement of a novel C-terminal kinase domain of Kir6.2 subunit in K-ATP channel rundown reactivation. *J. Mol. Model.* **7**, 20-25.

(24) Lou, K.-L., Huang, P.-T., Shiau, Y.-S. and Shiau, Y.-Y. (2002) Molecular determinants of hanatoxin binding in voltage-gated potassium channel *drk1*. *J. Mol. Recognit.* **15**, 175-179.

(25) Chia, J.-S., Shiau, Y.-S., Huang, P.-T., Shiau, Y.-Y., Lou, K.-L. (2003) Structural analysis of the influence of enzyme activity by surface peptide Gtf-P1 in *S. mutans* glucosyltransferase GtfC. *J. Mol. Model.* DOI 10.1007/s00894-003-0121-5.

(26) Hahn, M. (1995) Receptor surface models. 1. Definition and constructions. *J. Med. Chem.* **38**, 2080-2090.

(27) Hahn, M. and Rogers, D. (1995) Receptor surface models. 2. Application to quantitative structure-activity relationships studies. *J. Med. Chem.* **38,** 2091-2102.

(28) Costantino, G., Macchiarulo, A., Camaioni, E., and Pellicciari, R. (2001) Modeling of poly-(ADP-ribose)-polymerase (PARP) inhibitors: docking of ligands and quantitative structure-activity relationship analysis. *J. Med. Chem.* **44,** 3786-3794.

(29) Li-Smerin, Y. and Swartz, K. J. (1998) Gating modifier toxins reveal a conserved structural motif in voltage-gated Ca^{2+} and K^{+} channels. *Proc. Natl. Acad. Sci. USA* **95**, 8585-8589.

(30) Ruta, V., Jiang, Y., Lee, A., Chen, J., and MacKinnon, R. (2003) Functional analysis of an archaebacterial voltage-dependent K^{+} channel. *Nature* **422**, 180-185.

(31) Jiang, Y., Lee, A., Chen, J., Ruta, V., Cadene, M., Chait, B. T., and MacKinnon, R. (2003) X-ray structure of a voltage-dependent K^{+} channel. *Nature* **423**, 33-41.

(32) Jiang, Y., Ruta, V., Chen, J., Lee, A., and MacKinnon, R. (2003) The principle of gating charge movement in a voltage-dependent K^{+} channel. *Nature* **423**, 42-48.

(33) Takeuchi, K., Park, E. J., Lee, C. W., Kim, J. I., Takahashi, H., Swartz, K. J., and Shimada, I. (2002) Solution structure of ω-Grammotoxin SIA, a gating modifier of P/Q and N-type Ca^{2+} Channel. *J. Mol. Biol.* **321**, 517-526.

(34) Terras, F. R., Eggermont, K., Kovaleva, V., Raikhel, N. V., Osborn, R. W., Kester, A., Rees, S. B., Torrekens, S., van Leuven, F., and Vanderleyden, J. (1995) Small cysteine-rich antifungal proteins from radish: their role in host defense. *Plant Cell* **7**, 573-588.

(35) Froy, O. and Gurevitz, M. (1998) Membrane potential modulators: a thread of scarlet from plants to humans. *FASEB J.* **12**, 1793-1796.

(36) Hwa, V., Oh, Y., and Rosenfeld, R. G. (1999) Insulin-like growth factor binding proteins: a proposed superfamily. *Acta Paediatrica Suppl.* **88**, 37-45.

(37) Boisbouvier, J., Blackledge, M., Sollier, A., and Marion, D. (2000) Simultaneous determination of disulphide bridge topology and three-dimensional structure using ambiguous intersulphur distance restraints: possibilities and limitations. *J. Biomol. NMR* **16**, 197-208.

(38) Fariselli, P. and Casadio, R. (2001) Prediction of disulfide connectivity in proteins. *Bioinformatics* **17**, 957-964.

(39) Higgins, D., Thompson, J., Gibson, T., Thompson, J. D., Higgins, D. G., and Gibson, T. J. (1994) CLUSTAL W: improving the sensitivity of progressive multiple sequence alignment through sequence weighting, position-specific gap penalties and weight matrix choice. *Nucleic Acids Res*. **22**, 4673-4680.

(40) Hall, T. A. (1999) BioEdiit: auser-friendly biological sequence alignment editor and analysis program for Window 95/98/NT. *Nucleic Acids Symposium Series* **41**, 95-98.

(41) Gonzalez, C., Roseman, E., Bezanilla, F., Alvarez, O., and Latorre, R. (2000) Modulation of the shaker K^+ channel gating kinetics by the S3-S4 linker. *J. Gen. Physiol.* **115**, 193-207.